Influence of growth conditions from metalorganic compounds on the preparation of *n*-CdTe epitaxial layers using isopropyl iodide

© A.N. Moiseev, V.S. Evstigneev, A.V. Chilyasov¶, M.V. Kostunin

Devyatykh Institute of Chemistry of High-Purity Substances Russian Academy of Sciences,
603951 Nizhny Novgorod, Russia

¶ E-mail: chil@ihps-nnov.ru

Received November 12, 2021
Revised November 15, 2021
Accepted November 15, 2021

The dependence of iodine incorporation in CdTe layers on the deposition conditions during metalorganic vapor phase epitaxy is investigated. The growth of the layers was carried out from dimethylcadmium and diethyltellurium in the hydrogen flow in a vertical reactor with a hot wall condition at a total pressure of 20 kPa. The total iodine concentration was determined by secondary ion mass spectrometry, the electrically active concentration was determined from the Hall effect measurement. The iodine incorporation depends on the crystallographic orientation of the substrate (were studied (100), (310), (111)A, (111)B, (211)A and (211)B), the concentration of the doping precursor (flux range $5 \cdot 10^{-8}-3 \cdot 10^{-6}$ mol/min), the mole ratio of organometallic compounds (DMCd/DETe = 0.25−4), growth temperature (335−390°C) and the walls of the reactor above the pedestal (hot wall zone 290−320°C). The total iodine concentration reached $5 \cdot 10^{18}$ cm^{-3} and the activation efficiency was $\sim$ 4%. After thermal annealing in cadmium vapor at 500°C the activation efficiency was $\sim$ 100%.

Keywords: epitaxial layers, metalorganic vapour phase epitaxy, CdTe, iodine doping, isopropyl iodide, thermal annealing.

DOI: 10.21883/SC.2022.03.53068.9767

1. Introduction

Cadmium telluride is used in γ-ray and X-ray high-sensitivity detectors, thin-film solar cells and other optoelectronic devices [1,2]. In addition, CdTe has a close lattice parameter with $Hg_{1-x}Cd_xTe$ and therefore it is used as a buffer layer for epitaxy of large-area $Hg_{1-x}Cd_xTe$ layers on alternative substrates such as Si and GaAs [3–6].

To ensure application of semiconductor devices for manufacturing purposes, a material with *n*- and *p*-type conductivity and controlled electrophysical properties is required. For example, *p*-CdTe with hole concentration $\geq 10^{16}$ cm^{-3} is required for efficient solar cells, and [7,8] demonstrated the ability to produce arsenic-doped CdTe layers with $p(T_{room}) = (1-2) \cdot 10^{17}$ cm^{-3} using a metalorganic vapor phase epitaxy (MOVPE). At the same time, *p*-CdTe/*n*-CdTe/n^+-Si based X-ray and γ-ray detectors require high-alloy *n*-CdTe [9]. Iodine and indium are most widely used as *n*-type dopants for CdTe epitaxy. However, iodine is more preferable because of its lower diffusion coefficient in CdTe. It should be also noted that indium alkyls in MOVPE react with Te alkyls and form low-volatile adducts that lead to equipment memory effects. At the same time, the use of iodine alkyls does not lead to memory effects [6]. For chemical vapor deposition of CdTe, ethyl iodide [6,9–11], isopropyl iodide and n-butyl iodide are used for $Hg_{1-x}Cd_xTe$ deposition [12,13]. As compared with ethyl iodide, the two latter precursors have lower thermal resistance and lower saturated vapor pressure which makes additive dosing more simple at low layers doping level.

Iodine in CdTe is a shallow donor with ionization energy 10−15 MeV derived from temperature dependence of hall measurements and photo luminescence [9,14,15]. In order to enable donor properties in iodine, iodine shall occupy the tellurium sublattice vacancies (I_{Te}). Therefore, CdTe layer synthesis shall be preformed in cadmium excess that will result in increased tellurium vacancy concentration (V_{Te}) and, respectively, to increased iodine concentration in the layers. In addition, CdTe growth in cadmium excess facilitates lower cadmium vacancy concentration (V_{Cd}) that can compensate for iodine by forming $V_{Cd}-I_{Te}$ complexes.

CdTe doping with ethyl iodide in MOVPE was investigated in several publications [9–11]. In [9], CdTe growth was obtained from dimethylcadmium (DMC), diethyltellurium (DET) and diisopropyltellurium (DIPT) in a vertical reactor. Deposition was carried out on GaAs (100) substrates within the range of 300−450°C with the reactor wall above the pedestal heated up to 200−300°C and atmospheric pressure. DET/DMC and DIPT/DMC molar ratios were fixed and equal to 0.5. Electron concentration in the layers were increased with growth temperature decrease from 425 to 325°C. Doped layers deposited from DET had a higher electron concentration than the layers grown using DIPT. Maximum electron concentration was equal to $2.6 \cdot 10^{18}$ cm^{-3} at substrate and reactor wall temperature 325 and 250°C, respectively. In [10], deposition was performed from DMC, DET and ethyl iodide vapors on n^+-Si (211) substrates in the temperature range of 325−450°C and at atmospheric pressure. DET/DMC molar ratio was changed from 0.05 to 0.3. Electron concentration was gradually increased with DET/DMC ratio decrease.

The highest electron concentration was $2.5 \cdot 10^{18}\,\mathrm{cm}^{-3}$ in the layers obtained at DET/DMC = 0.05 and substrate temperature 400°C.

In [11], when $n-p$-homojunction was provided for n-CdTe/p-CdTe/ZnTe/GaAs (100) solar cells, the authors used the MOVPE method with CdTe arsenic hydride doping and ethyl iodide doping in a vertical reactor with cold walls. n-CdTe was deposited at 100 and 500 Torr from DMC and DIPT (DMC/DIPT = 1–7) vapors at 250, 300 and 400°C. CdTe layer properties were highly dependent on the deposition conditions. The highest free electron concentration $4.5 \cdot 10^{16}\,\mathrm{cm}^{-3}$ (without additional annealing at 550°C in cadmium atmosphere) was obtained during layer deposition at 250°C, reactor pressure 500 Torr and DMC/DIPT = 7. Comparison of total iodine content (secondary ion mass spectrometry (SIMS) method) with free electron concentration (hall measurement) in layers has shown that the iodine activation degree was 25–30% at a deposition temperature from 250 to 300°C.

The literature data review has revealed that iodine dopant incorporation into CdTe and its electrical behavior are heavily dependent on the preparation conditions, and the use of compounds with lower thermal resistance than ethyl iodide for CdTe doping in MOVPE was not investigated.

In this study, we investigated the patterns of iodine incorporation in MOVPE CdTe from isopropyliodide and its electrical activity depending on the substrate crystal-lattice orientation, doping precursor concentration, metalorganic compound ratios, growth and reactor wall temperatures, as well as influence of subsequent thermal annealing on the charge carrier concentration in the layers.

2. Experimental procedure

CdTe layers were grown in a vertical silica reactor with above-pedestal preheating zone ($T_{\mathrm{prezon}} = 290–320$°C) at a total pressure of 20 kPa and substrate temperature $T_{\mathrm{subs}} = 335–390$°C (internal resistance heater). DMC and DET, respectively, were used as the sources of cadmium and tellurium. Iodine doping of layers was carried out using isopropyliodide (IPI). DMC and DET purity was at least 99.999%, IPI purity was at least 98%. During CdTe layer deposition, DET (V_{DETe}) and DMC (V_{DMCd}) flows were changed from $4 \cdot 10^{-5}$ to $1.6 \cdot 10^{-4}$ mole/min, and DMC/DET at reactor inlet was changed from 0.25 to 4. IPI flow rate (V_{IPI}) was variated from $5 \cdot 10^{-8}$ to $3 \cdot 10^{-6}$ mole/min. Chemicals were injected into the reactor via separate tubes in a hydrogen flow purified by diffusion through a palladium filter. Total hydrogen flow rate into the reactor was equal to 3 l/min (in normal conditions). For growth, „epiready" substrates of semi-insulating GaAs with crystal-lattice orientations (100)4° → ⟨110⟩, (310), (111)(A and B) and (211)(A and B) were used. Before deposition, the substrates were annealed in hydrogen flow at 550°C during 15 min in order to remove the natural oxide layer. To avoid substrate component diffusion into the doped layer, a $2–3\,\mu$m CdTe buffer layer was initially applied to the substrates.

CdTe layer thickness with error 5% was calculated from interference curves obtained using Nicolet 6700 Fourier spectrometer. Infrared spectra of layers were recorded at 298 K within $500–6000\,\mathrm{cm}^{-1}$ with a resolution of $0.5\,\mathrm{cm}^{-1}$. Iodine concentration profile by CdTe layer thicknesses was investigated using SIMS method. For SIMS spectra recording, a time-of-flight secondary ion mass spectrometer TOF.SIMS-5 was used. Concentration profiles were obtained using ion pulsed beam Bi_3^+ with energy 25 keV (current 1 pA, grid $30 \times 30\,\mu$m) for analysis and Cs^+ with energy 1 keV (grid $150 \times 150\,\mu$m) for spraying. Ion ^{127}I lines and noise signal from ^{126}Te and ^{128}Te lines were recorded. Specified iodine content in layers was defined by the relationship between the line intensity difference and CdTe cluster line intensity. Iodine assay content was measured using inductively coupled plasma atomic emission spectrophotometry (relative error is 5%).

Dark electrophysical parameters of CdTe layers with error 20% were derived from hall measurements using Van der Pauw method in a permanent magnetic field of 0.5 T at room temperature. Doped layer thicknesses for electrophysical measurements were at least $3\,\mu$m. Indium was used to provide ohmic contacts to n-CdTe.

Crystal-lattice orientation and structural perfection of layers were defined using rocking curve half-width (FWHM) by a double-crystal X-ray diffraction method in DRON-4M device.

To increase the fraction (concentration) of electrically active iodine, high-temperature annealing of CdTe was carried out in cadmium vapor within the range of 400–600°C during 3 h. Weighed Cd and CdTe samples were put into a quartz vessel and vacuum treated and then charged into a two-zone furnace. A temperature in the weighed Cd zone was lower than the sample zone temperature by 10°C. For correct interpretation of iodine doped CdTe layers, comparison with undoped samples grown and annealed in similar conditions was used.

3. Experimental results and discussion

To investigate the iodine dopant incorporation in the epitaxial CdTe layers, a range of orientations was extended herein, but the main attention was drawn to CdTe(100) layers like in other publications. Table 1 provides some properties of CdTe layers, whose orientation always matched the substrate orientation, that were obtained in a single process. All layer properties listed in the table are distinctly dependent on the orientation. Surface morphology of the samples was changed from a mirror surface for (100) and (310) orientations to opaque surface for (111)A and (211)A orientations, the best rocking curve half-width was observed in CdTe (211)A sample. Free (noncompensated) electron concentration is maximum in CdTe (211)A ($1.1 \cdot 10^{16}\,\mathrm{cm}^{-3}$) layers.

Table 1. Some properties of heteroepitaxial layers of CdTe:I/CdTe/GaAs with various crystal-lattice orientation deposited in a single process ($T_{subs} = 350°C$, $T_{prezon} = 300°C$, $V_{DMCd} = V_{DETe} = 4 \cdot 10^{-5}$ mole/min, $V_{IPI} = 1 \cdot 10^{-6}$ mole/min)

Property	Orientation					
	(100)	(310)	(111)B	(111)A	(211)B	(211)A
Surface	Mirror	Mirror	Mirror	Very opaque	Mirror and opaque	Opaque
FWHM, ang. min	7.4	6.1	11.1*	6.4**	3.6	1.9
n_{room}, cm^{-3}	$5.4 \cdot 10^{15}$	$6.6 \cdot 10^{14}$	$2.3 \cdot 10^{12}$	$8.5 \cdot 10^{12}$	$1 \cdot 10^{12}$	$1.1 \cdot 10^{16}$
μ_{room}, $cm^2/(B \cdot c)$	240	70	110	90	370	330

Note. * Twins are available (~ 50%). ** Twins are available (~ 20%).

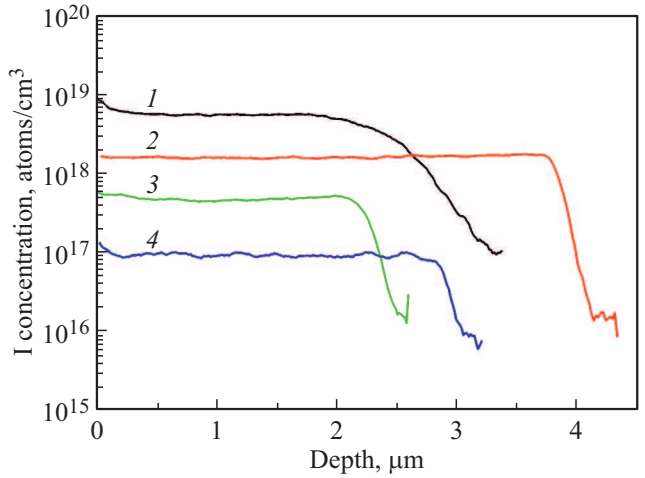

Figure 1. Iodine concentration distribution over the CdTe layer thicknesses with various crystal-lattice orientation that were grown in a single process: *1* — (111)A, *2* — (111)B, *3* — (310), *4* — (100). ($T_{subs} = 350°C$, $T_{prezon} = 300°C$, DMC/DET = 1, $V_{DMCd} = 4 \cdot 10^{-5}$ mole/min, $V_{IPI} = 5 \cdot 10^{-7}$ mole/min).

Iodine incorporation in CdTe also depends to a great extent on the crystal-lattice orientation of the growing layer (Fig. 1). The orientation effect of dopant incorporation has been already observed in earlier studies during vapor phase doping of $A^{III}B^{V}$ compound layers [16,17], as well as during arsenic doping of $Hg_{1-x}Cd_xTe$ and CdTe layers [3,18]. The maximum iodine incorporation $\sim 5 \cdot 10^{18}$ cm^{-3} is observed for (111)A orientation (Fig. 1) that is higher than for (100) orientation by almost a factor of 2. Iodine concentration in CdTe layers with various crystal-lattice orientation is increased in the series (100) < (310) < (111)B < (111)A. However, the CdTe layer growth rate in various planes is decreased in the series (111)B > (100) > (310) ~ (111)A. Different growth rate at surfaces with different orientation is due to surface process kinetics and is defined by different geometry of bonds between absorbed atoms and surface with more advantageous growth kinetics at (111)B orientation. However, iodine incorporation in CdTe in these conditions is not correlated with the growth rate. Iodine incorporation in CdTe shall be considered as a process competing with Te incorporation. Since (111)B surface is Te-enriched and (111)A surface is Cd-enriched, than there are more tellurium vacancies on (111)A orientation surface that can be occupied by iodine. In addition, a doping compound decomposition process [19] and iodine desorption from the surface may significantly contribute to the dopant incorporation in the layer. For each CdTe orientation, contribution of these stages in the iodine incorporation into the layer may be different and depends on other growth conditions, first of all on the substrate temperature and composition of gas-vapor mixture approaching the substrate.

Figure 2 shows iodine incorporation in CdTe (100) obtained with stationary IPI flow rate $5 \cdot 10^{-7}$ mole/min vs. DMC/DET molar ratio variation during a single deposition process (with stationary DMC flow rate). As shown in Fig. 2, iodine concentration in layers is steadily increased with increase in DMC/DET. Increased DMC/DET during the growth process results in increased tellurium vacancy concentration and higher probability of iodine incorporation into the tellurium sublattice.

Figure 3 shows the iodine concentration distribution in the CdTe layers obtained in a single process on (100) and (111)B orientation substrates with stepwise variation of the

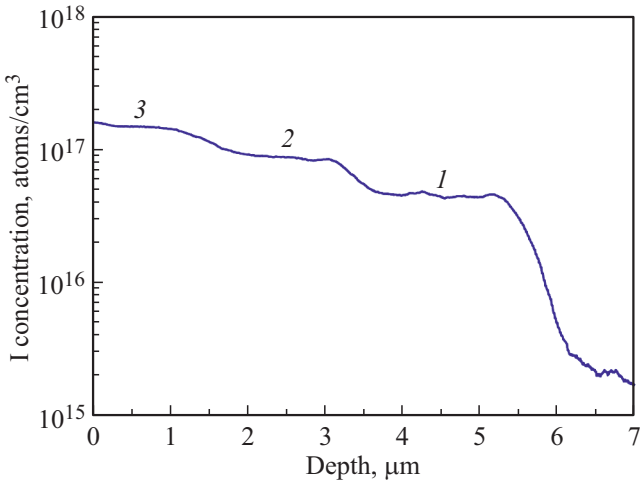

Figure 2. Iodine concentration distribution over the CdTe (100) thickness obtained with DMC/DET molar ratio variation during the deposition process: *1* — 0.5, *2* — 1, *3* — 1.4. ($T_{subs} = 350°C$, $T_{prezon} = 300°C$, $V_{DMCd} = 4 \cdot 10^{-5}$ mole/min, $V_{IPI} = 5 \cdot 10^{-7}$ mole/min).

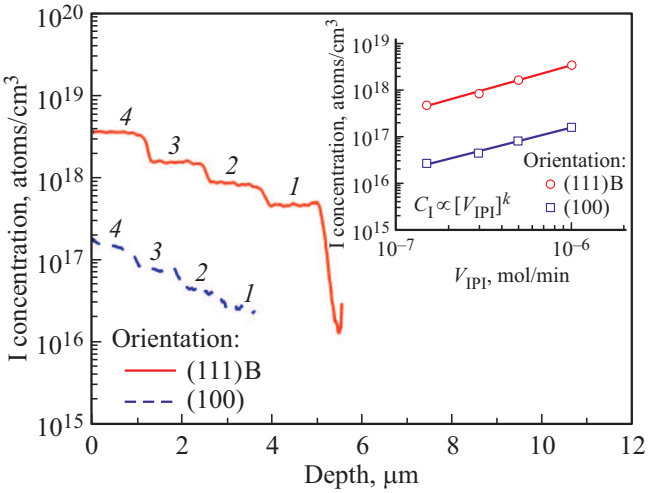

Figure 3. Iodine concentration distribution over the CdTe layer thicknesses with different crystal-lattice orientation that were grown in a single process with stepwise variation of V_{IPI}, mole/min: *1* — $1.5 \cdot 10^{-7}$, *2* — $3 \cdot 10^{-7}$, *3* — $5 \cdot 10^{-7}$, *4* — $1 \cdot 10^{-6}$; iodine incorporation in CdTe as function of IPI flow rate for (111)B and (100)4° → ⟨110⟩ orientations (see the detail). ($T_{subs} = 350$°C, $T_{prezon} = 300$°C, DMC/DET = 1, $V_{DMCd} = 4 \cdot 10^{-5}$ mole/min).

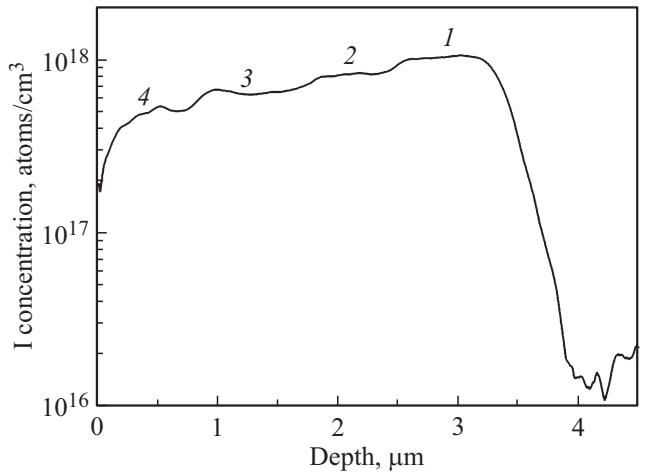

Figure 4. Iodine concentration distribution over the CdTe (310) thickness obtained with growth temperature variation during the deposition process, °C: *1* — 350, *2* — 365, *3* — 380, *4* — 390. ($T_{prezon} = 300$°C, DMC/DET = 1, $V_{DMCd} = 4 \cdot 10^{-5}$ mole/min, $V_{IPI} = 1 \cdot 10^{-6}$ mole/min).

IPI flow from $1.5 \cdot 10^{-7}$ to $1 \cdot 10^{-6}$ mole/min and with the sameDMC/DET molar ratio = 1. Increased IPI flow leads to increased iodine concentration in the layers. The iodine incorporation in CdTe layers with (100) and (111)B crystal-lattice orientations within the vapor phase IPI flow range of $1.5 \cdot 10^{-7}$–$1 \cdot 10^{-6}$ mole/min is increased in accordance with the following expression (see the detail in Fig. 3):

$$C_I\,(\text{at/cm}^3) \propto [V_{IPI}\,(\text{mol/min})]^k, \qquad (1)$$

where $k = 0.95$–$1.05\ (\pm 0.05)$.

Figure 4 shows the iodine incorporation in CdTe (310) obtained with stationary IPI flow rate $1 \cdot 10^{-6}$ mole/min vs. growth temperature variation from 350 to 390°C during deposition. As shown in Fig. 4, four doping steps can be clearly distinguished. The greatest iodine incorporation is observed at a growth temperature of 350°C. Gradual increase in the growth temperature up to 390°C leads to lower iodine concentration in the layer. We assume that the following two factors influence the decrease in iodine incorporation in CdTe with increased growth temperature: 1) increase in DET thermal decomposition degree and increase in Te/Cd on the surface; 2) increase in iodine desorption from the growth surface. A similar effect was observed during arsenic doping of CdTe [8] and in earlier investigations of vapor phase doping of $A^{III}B^{V}$ compounds [20].

The relationship of the iodine atom concentration and electrophysical parameters in the CdTe:I (100) layers vs. isopropyliodide flow rate (Table 2) was investigated. The free electron concentration in the layers reached its maximum $5.6 \cdot 10^{15}$ cm^{-3} at isopropyliodide flow rate $1 \cdot 10^{-6}$ mole/min. In terms quality, our findings replicate the data in [9] regarding the presence of maximum on an equivalent relationship, however, in terms of quantity, they differ evidently. This difference may be due to the difference in precursors, deposition conditions and reactor geometry. Comparison of the hall measurements with the iodine concentration in the layers (SIMS) shows that the degree of iodine electrical activity varies in the given conditions from ∼ 0.02 to ∼ 4% with a maximum also with $V_{IPI} = 1 \cdot 10^{-6}$ mole/min.

Table 2. Iodine concentration $C(\text{I})_{CdTe}$ (SIMS) and electrophysical parameters (n and μ) of CdTe:I (100) layers vs. doping compound flow rate V_{IPI} ($T_{subs} = 350$°C, $T_{prezon} = 300$°C, $V_{DMCd} = V_{DETe} = 4 \cdot 10^{-5}$ mole/min)

V_{IPI}, mol/min	$5 \cdot 10^{-8}$	$5 \cdot 10^{-7}$	$1 \cdot 10^{-6}$	$3 \cdot 10^{-6}$
$C(\text{I})_{CdTe}$, at/cm^3	$8.3 \cdot 10^{15}$	$7.7 \cdot 10^{16}$	$1.5 \cdot 10^{17}$	$4.3 \cdot 10^{17}$
n_{room}, cm^{-3}	$1.4 \cdot 10^{12}$	$7.4 \cdot 10^{14}$	$5.6 \cdot 10^{15}$	$2.2 \cdot 10^{15}$
μ_{room}, cv^2/(B · c)	420	480	240	310
Degree of activation I, %	0.017	0.96	3.7	0.51

Table 3. Free electron concentration and mobility in the CdTe:I (100) layers vs. vapor phase DMC/DET ($T_{subs} = 350$°C, T_{prezon}=300°C, V_{DETe}=$4 \cdot 10^{-5}$ mole/min, V_{IPI}=$5 \cdot 10^{-7}$ mole/min)

DMC/DET	0.25*	1	2	3
n_{room}, cm^{-3}	$\sim 1 \cdot 10^{12}$**	$7.4 \cdot 10^{14}$	$3 \cdot 10^{15}$	$1.8 \cdot 10^{15}$
μ_{room}, cm^2/(B · c)	–	480	540	200
Growth rate, μm/h	2.79	1.46	1.86	1.24

Note. * $V_{DMCd} = 4 \cdot 10^{-5}$ mol/min, V_{DETe}=$1.6 \cdot 10^{-4}$ mol/min.
** Resistivity assessment ($\rho \sim 10^4$ Ohm · cm).

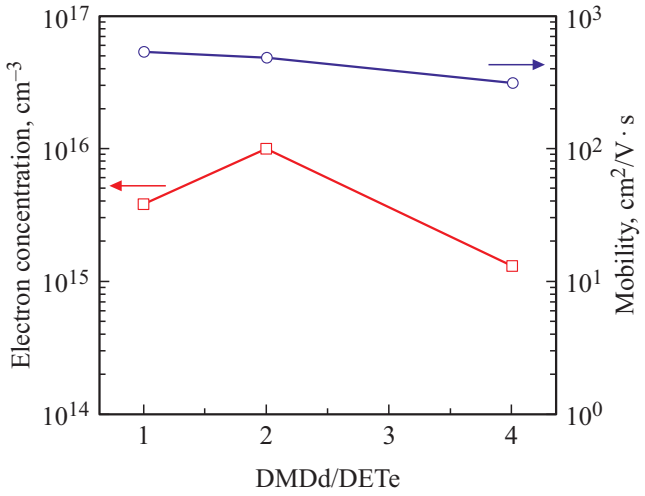

Figure 5. Free electron concentration and mobility in the CdTe:I (100) layers vs. vapor phase DMC/DET ratio ($T_{subs} = 350°C$, $T_{prezon} = 310°C$, $V_{DETe} = 4 \cdot 10^{-5}$ mol/min, $V_{IPI} = 1 \cdot 10^{-6}$ mol/min).

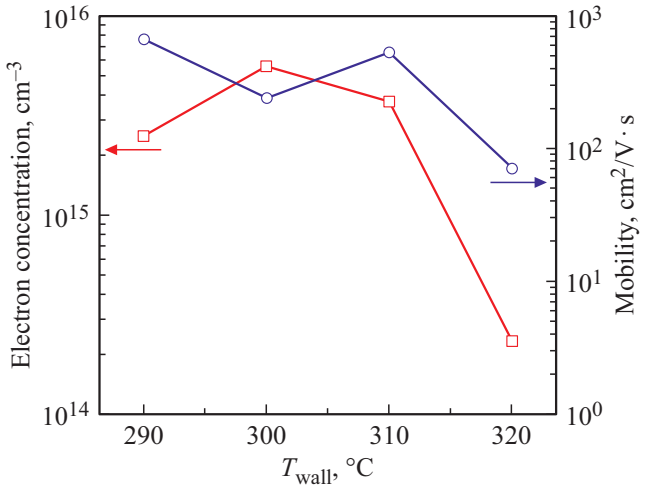

Figure 6. Free electron concentration and mobility in the CdTe:I (100) layers vs. reactor wall temperature ($T_{subs} = 350°C$, $V_{DMCd} = V_{DETe} = 4 \cdot 10^{-5}$ mol/min, $V_{IPI} = 1 \cdot 10^{-6}$ mol/min).

Table 3 shows the investigation findings regarding the influence of vapor phase DMC/DET on the electron concentration and mobility in the CdTe:I (100) layers.

In the tellurium excess, layers had high resistivity, at DMC/DET = 1 and above, electron concentration reached its maximum $3 \cdot 10^{15}$ cm^{-3} at DMC/DET = 2. Electron mobility behavior was the same. Vapor phase layer growth rate in the tellurium excess was evidently higher than in the cadmium excess. Increase in the doping compound flow rate by a factor of 2 exceeded the electron concentration in the maximum up to $9.8 \cdot 10^{15}$ cm^{-3} (Fig. 5), and for a (211)A orientation sample, $n = 3.6 \cdot 10^{16}$ cm^{-3} was achieved. In [10,11], where free electron concentration in CdTe:I (100) vs. vapor phase DMC/DET (DIPT) was investigated, no maximum on this relationship was observed.

In [9], rather sharp maximum was observed on the relationship of free electron concentration in the CdTe:I (100) layers vs. the temperature of the reactor heated walls at $T_{prezon} = 250°C$. Our investigation also showed a maximum (Fig. 6) on this relationship, but only at $T_{prezon} = 300-310°C$. The substrate temperature decrease below 350°C in our conditions did not resulted in the increased free electron concentration in the CdTe:I (100) layers (Table 4) like in [9–11]. Annealing of doped layers in the saturated cadmium vapor at 500°C during 3 h resulted in almost full activation of the iodine dopant as shown for CdTe:I (100) (Table 5).

We can explain the electrical behavior of iodine in the CdTe:I layers using a compensation model like in [9–11,21,22]. Iodine preferably occupies the tellurium vacancies in the CdTe (I_{Te}) lattice and forms a charged acceptor complex $[V_{Cd}^{2-} - I_{Te}^{+}]^{-}$ with cadmium vacancies. Electrically active iodine is compensated by reaction $[V_{Cd}^{2-} - I_{Te}^{+}]^{-} + I_{Te}^{+}$. The higher the cadmium vacancy concentration is, the higher the complex concentration is and, thus, the higher the compensation effect is.

Cd/Te may be different in the vapor phase and in the growing layer surface and depends on the thermal resistance of the precursors and deposition conditions. Dimethylcadmium is almost completely decomposed in the hydrogen flow at 350°C with decomposition started at $\sim 250°C$ [23]. Diethyltellurium decomposition starts in an equimolar mixture with dimethylcadmium at 330–350°C and almost total decomposition takes place at $> 400°C$ [24]. A heterogeneous factor (surface vs. volume) has a great influence on the degree of DMC decomposition (much

Table 4. Electron concentration and mobility in layers vs. CdTe:I (100) growth temperature ($T_{prezon} = 310°C$, $V_{DMCd} = 8 \cdot 10^{-5}$ mol/min, $V_{DETe} = 4 \cdot 10^{-5}$ mol/min, $V_{IPI} = 1 \cdot 10^{-6}$ mol/min)

T_{grow}, °C	335	350	365
n_{room}, cm^{-3}	$1.2 \cdot 10^{15}$	$9.8 \cdot 10^{15}$	$2.7 \cdot 10^{13}$
μ_{room}, cm^2/(B · c)	90	480	60
Growth rate, μm/h	1.58	1.9	1.95

Table 5. Electrophysical parameters of the CdTe layers before and after cadmium vapor annealing during 3 h

Annealing conditions	Charge carrier concentration n, cm^{-3}		Degree of activation I, %
	CdTe (100) undoped	CdTe (100):I $C(I) = 9\,10^{16}$ cm^{-3}	
Initial	High-resistivity	$8.0 \cdot 10^{14}$	0.9
400°C	High-resistivity	$5.2 \cdot 10^{16}$	58
500°C	$3.6 \cdot 10^{15}$	$8.9 \cdot 10^{16}$	95*
600°C	$1.7 \cdot 10^{16}$	$8.3 \cdot 10^{16}$	73*

Note. * Including the influence of intrinsic defects after annealing.

weaker for DET). A pre-decomposition zone (T_{prezon}) upstream of the pedestal leads to a greater degree of decomposition of metalorganic compounds (MOC) and changes Cd/Te in the flow approaching the substrate. Quantitative variation of the vapor phase composition depends on the temperature T_{prezon} and time of vapor phase molecules exposure to the chemical agent when the mixture moves from the pre-composition zone to upstream of the pedestal and this, in its turn, depends on the linear flow rate and reactor geometry. Most of authors do not provide such data of the used reactor. Differences in growth conditions and reactor geometry may result in different iodine incorporation and behavior in CdTe.

The CdTe layers with different crystal-lattice orientation are characterized by different concentration of inherent defects, and the iodine dopant is included in them and behaves differently which is proved by the obtained findings (Table 1 and Fig. 1). Increased flow rate of the doping compound, all other conditions being equal, results in the increased amount of iodine incorporated in the layer (see the detail in Fig. 3 and Table 2). Free electron concentration in the layers is also increased (Table 2). Achievement of the maximum by the electrons may be explained by penetration of many iodine atoms in other semiconductor lattice vacancies, except for I_{Te}, (complexes, voids, I_{Cd}, etc.) that compensate the dopant or neutral ones. The degree of iodine compensation also achieves the maximum (Table 2).

Vapor phase DMC/DET is an important factor influencing the Cd/Te on the growth surface. The CdTe deposition in the DMC excess leads to reduction of the amount of $[V_{Cd}^{2-} - I_{Te}^{+}]^{-}$ complexes in the layers, lower degree of I_{Te}^{+} compensation and higher concentration of free electrons (Table 3 and Fig. 5). The presence of the maximum on the relationship of n vs. DMC/DET at DMC/DET = 2 may be, for example, explained by increased vapor phase interaction between DMC (at $V_{DMCd} > 4 \cdot 10^{-5}$ mole/min) and IPI (at $V_{IPI} > 1 \cdot 10^{-6}$ mole/min) with a premature deposition CdI_2 ($T_{subs} = 388°C$) onto the reactor walls above the pedestal and by the reduction of actual Cd/Te on the growth surface. Lower Cd/Te results in lower incorporation of iodine into I_{Te}^{+} position and lower concentration of free electrons.

Zone temperature above the pedestal (T_{prezon}) influences the thermal decomposition of DMC in the range of 290−320°C and has no evident influence on the DET decomposition that changes actual Cd/Te on the growth surface leading to the occurrence of the maximum on the relationship of n vs. T_{prezon} (Fig. 6).

At the substrate temperature of 350°C in our deposition conditions, the best Cd/Te ratio on the growth surface and IPI decomposition degree are apparently provided owing to which the maximum occurs on the relationship of free electron concentration vs. T_{grow} (Table 4).

During annealing of doped layers at 500°C in cadmium vapor, cadmium vacancies are populated, $[V_{Cd}^{2-} - I_{Te}^{+}]^{-}$ complexes are destroyed and coupled I_{Te}^{+} donors are released, thus, approaching the iodine activation to 100% (Table 5). Comparison with the annealing result of undoped CdTe in the same conditions shows that the electron concentration in a doped sample depends, firstly, on the ionized iodine rather than on the interstitial cadmium.

4. Conclusion

We have investigated the patterns of iodine incorporation in MOVPE CdTe from isopropyliodide depending on the substrate crystal-lattice orientation, doping precursor concentration, metalorganic compound ratios, growth and reactor wall temperatures, as well as influence of subsequent thermal annealing on the charge carrier concentration in the layers. The crystal-lattice orientation of the layers has a strong impact on the iodine incorporation and behavior. When the doping precursor flow rate is increased, the total incorporation of the dopant in the layers and the concentration of electrically active iodine grow. Each orientation is characterized by its own set of inherent defects and iodine dopant that interacts with this set is distributed among the various lattice vacancies in a different way. The investigation in the given deposition conditions has identified the maxima on the relationships of free electron concentrations in the layers vs. isopropyliodide flow, DMC/DET, and pre-cracking zone and substrate temperatures. A noncompensated electron concentration in the CdTe (100) layers of $1.1 \cdot 10^{16}\,cm^{-3}$ and CdTe (211)A layers of $3.6 \cdot 10^{16}\,cm^{-3}$ has been achieved. The iodine activation degree was from ~ 0.02 to $\sim 4\%$. Upon cadmium-vapor annealing at 500°C during 3 h, the iodine activation degree in the CdTe layers was increased up to $\sim 100\%$.

Funding

The research was carried out under the state assignment of the Ministry of Education and Science of the Russian Federation (topic No. FFRN-2019-0004).

Acknowledgments

We would like to express our gratitude to M.N. Drozdov for SIMS investigations of layers and to I.I. Evdokimov for layer analysis using a ICP AE method.

Conflict of interest

The authors declare that they have no conflict of interest.

References

[1] C. Szeles. Phys. Status Solidi B, **241** (3), 783 (2004).
[2] J.M. Burst, J.N. Duenow, D.S. Albin, E. Colegrove, M.O. Reese, J.A. Aguiar, C.-S. Jiang, M.K. Patel, M.M. Al-Jassim, D. Kuciauskas, S. Swain, T. Ablekim, K.G. Lynn, W.K. Metzger. Nature Energy, **1** (3), 1 (2016).
[3] V.S. Evstigneev, A.V. Chilyasov, A.N. Moiseev, M.V. Kostyunin. Neorg. mater., **55** (10), 1040 (2019) (in Russian).

[4] V.S. Evstigneev, V.S. Varavin, A.V. Chilyasov, V.G. Remesnik, A.N. Moiseev, B.S. Stepanov. FTP, **52** (6), 554 (2018) (in Russian).
[5] R. Sporken, S. Sivananthan, K.K. Mahavadi, G. Monfroy, M. Boukerche, J.P. Faurie. Appl. Phys. Lett., **55** (18), 1879 (1989).
[6] C.D. Maxey, J.P. Camplin, I.T. Guilfoy, J. Gardner, R.A. Lockett, C.L. Jones, P. Capper, M. Houlton, N.T. Gordon. J. Electron. Mater., **32** (7), 656 (2003).
[7] A.V. Chilyasov, A.N. Moiseev, V.S. Evstigneev, B.S. Stepanov, M.N. Drozdov. Neorg. mater., **52** (12), 1284 (2016) (in Russian).
[8] V.S. Evstigneev, A.V. Chilyasov, A.N. Moiseev, M.V. Kostunin. TSF, **689**, 137514 (2019).
[9] K. Yasuda, Y. Tomita, Y. Masuda, T. Ishiguro, Y. Kawauchi, H. Morishita, Y. Agata. J. Electron. Mater., **31** (7), 785 (2002).
[10] M. Niraula, K. Yasuda, R. Torii, Y. Higashira, R. Tamura, B.S. Chaudhari, T. Kobayashi, H. Goto, S. Fujii Y. Agata. J. Electron. Mater., **49** (11), 6996 (2020).
[11] P.Y. Su, R. Dahal, G.C. Wang, S. Zhang, T.M. Lu, I.B. Bhat. J. Electron. Mater., **44** (9), 3118 (2015).
[12] S. Murakami, T. Okamoto, K. Maruyama, H. Takigawa. Appl. Phys. Lett., **63** (7), 899 (1993).
[13] M. Niraula, T. Aoki, Y. Nakanishi, Y. Hatanaka. J. Cryst. Growth, **200** (1), 90 (1999).
[14] D. Brun-Le-Cunff, T. Baron, B. Daudin, S. Tatarenko, B. Blanchard. Appl. Phys. Lett., **67** (7), 965 (1995).
[15] N.C. Giles, J. Lee, D. Rajavel, C.J. Summers. J. Appl. Phys., **73** (9), 4541 (1993).
[16] R. Bhat, C. Caneau, C.E. Zah, M.A. Koza, W.A. Bonner, D.M. Hwang, S.A. Schwarz, S.G. Menocal, F.G. Favire. J. Cryst. Growth, **107**, 772 (1991).
[17] M. Kondo, C. Anayama, T. Tanahashi, S. Yamazaki. J. Cryst. Growth, **124**, 449 (1992).
[18] V.S. Evstigneev, A.V. Chilyasov, A.N. Moiseev, S.V. Morozov, D.I. Kuritsyn. FTP, **55** (1), 9 (2021) (in Russian).
[19] G.B. Stringfellow. J. Cryst. Growth, **75** (1), 91 (1986).
[20] D.V. Forbes, J.J. Coleman. MRS Online Proceedings Library (OPL), **340**, 289 (1994).
[21] S. Seto, A. Tanaka, Y. Masa, M. Kawashima. J. Cryst. Growth, **117**, 271 (1992).
[22] Y. Marfaing. TSF, **387**, 123 (2001).
[23] J.E. Hails, D.J. Cole-Hamilton, W. Bell. J. Cryst. Growth, **145**, 596 (1994).
[24] J.B. Mullin, S.J.C. Irvine, D.J. Ashen. J. Cryst. Growth, **55**, 92 (1981).